Risk-Based Optimal Operation of Coordinated Natural Gas and Reconfigurable Electrical Networks with Integrated Energy Hubs

Hemmati , Mohammad ; Abapour, Mehdi; Mohammadi-ivatloo, Behnam; Anvari-Moghaddam, Amjad

Published in:
IET Renewable Power Generation

DOI (link to publication from Publisher):
10.1049/rpg2.12189

Publication date:
2021

Document Version
Publisher's PDF, also known as Version of record

Received: 26 August 2020 | Revised: 3 March 2021 | Accepted: 18 April 2021

DOI: 10.1049/rpg2.12189

IET Renewable Power Generation

The Institution of Engineering and Technology WILEY

ORIGINAL RESEARCH PAPER

Risk-based optimal operation of coordinated natural gas and reconfigurable electrical networks with integrated energy hubs

Mohammad Hemmati[1] | **Mehdi Abapour**[1] | **Behnam Mohammadi-Ivatloo**[1,2] | **Amjad Anvari-Moghaddam**[1,2]

[1] Faculty of Electrical and Computer Engineering, University of Tabriz, Tabriz, Iran

[2] Department of Energy Technology, Aalborg University, Aalborg 9220, Denmark

Correspondence
Behnam Mohammadi-Ivatloo, Faculty of Electrical and Computer Engineering, University of Tabriz, Tabriz, Iran.
Email: bmohammadi@tabrizu.ac.ir

Funding information
University of Tabriz, Grant/Award Number: 3622; Iran National Science Foundation (INSF), Grant/Award Number: 99012662

Abstract

This paper elaborates on optimal scheduling of coordinated power and natural gas (NG) networks in the presence of interconnected energy hubs considering reconfiguration as a flexibility source. With regard to the energy hub system consisting of several generation units, storage and conversion technologies, as well as natural gas-fired units, the high interdependency between gas and electricity carriers should be captured. The hourly reconfiguration capability is developed for the first time in a multi-energy system to enhance the optimal power dispatch and gas consumption pattern. The realistic interdependency of electrical and NG grids is investigated by employing the steady-state Weymouth equation and AC-power flow model for power and gas networks, respectively. Furthermore, to handle the risk associated with strong uncertainty of wind power, load, and real-time power price, the conditional value at risk approach is employed. The proposed model is implemented on the integrated test system and simulation results are presented for different cases. The impact of the risk aversion level on operating cost and optimal scheduling of controllable units is examined. Numerical results demonstrate that reconfigurable capability reduces the operational cost up to 7.82%.

1 | INTRODUCTION

1.1 | Motivation

Natural gas (NG) plays a significant role in energy supply prospects around the world. For example, the share of NG in total US energy consumption has increased from 21% by 1980 to 27% by 2012, and it is anticipated that by 2040, over 35% of total energy production in this country is provided by NG [1]. The emergence of natural gas-fired (GF) generators, combined heat and power (CHP) units have led to the utilization of NG as the primary fuel for electricity production. In addition to the interdependency between electricity and NG systems, the optimal behaviour of units per hour is limited to various technical and economic limitations that lead to fluctuations in gas consumption by these sources. Fluctuations in the NG consumption pattern could negatively affect the gas flow in pipelines and pressure in different gas nodes, which may endanger the safety of the NG network. They could also put the safe operation of GF units and ultimately the reliability of power grid at risk. Meanwhile, the energy hub (EH) as a fundamental concept of multi-carrier energy systems (MCES) can be considered as a promising solution that is connected to different buses and gas nodes to supply electrical and thermal loads, locally [2]. Because of the various paths in the EH to meet multiple consumers, the optimal performance of existing equipment to minimize total system costs should be captured. Furthermore, providing a flexible configuration is a suitable and cost-effective solution that provided multiple benefits to utility and consumers, such as power loss and operation cost minimization, as well as reliability improvement. The hourly optimal topology is accessible by opening and closing tie-switches through the reconfiguration process [3]. Such actions can change the dispatch portfolio of GF units, and the gas flow accordingly. In addition to the complexity of scheduling MCES, the optimal operation of coordinated electrical and NG networks involves uncertainty

associated with RES power output, load demand, and energy prices.

Toward the goals of coordinated power and NG networks scheduling in reliable and economical ways have been studied recently, an essential challenge of the integrated power and NG systems is to derive the comprehensive model of risk-based operation of the reconfigurable electrical network coupled with NG system, through emerging facilities such GF units and interconnected EHs. This model should tackle RES generation, load, and energy price variation, as well as all interactions and constraints between two networks.

1.2 | Literature review and related works

The fast-growing utilization of natural gas as the primary fuel for electricity generation has led researchers to focus on modelling and operation of the NG network. The flow of NG into gas pipes is a complex phenomenon that requires the use of partial differential equations to well represents its behaviour [4],[5]. To simplify these complex equations, several assumptions are considered, resulting in equation analysis in a steady-state or transient state. A dynamic programming approach was presented in [6] to minimize the operation cost of long NG pipelines including a pressure regulating stations. In [7], a bi-level optimization approach was introduced to solve the optimal location and determination problem for pipeline diameter, which was formulated as a mixed-integer non-linear programming (MINLP) model.

Recently, GF units with their unique features such as higher efficiency, fast response, far less pollution generation, and quick start-up have triggered more dependence of the electricity grid to the NG network. Therefore, the electricity sector has become an important player in the gas industry, which has led to a strong interaction between electricity and NG networks. In contrast, the gas price variability, and its effects on the power system should be accounted for coordinated scheduling of power and gas networks. Authors in [8] evaluated the robust flexible security constraint unit commitment (SCUC) model for interconnected multi-carrier energy networks n the presence of flexible resources. The coordinated optimal energy dispatch of integrated electricity and NG networks under the stochastic optimization approach was extended by [9],[10]. In [11], a bi-level optimization problem was proposed for optimal scheduling of integrated NG and electricity grids with respect to NG transient state equations. The security constrained integrated electrical and NG networks co-expansion planning integrated with demand response and high penetration of wind energy was evaluated by [12]. The expansion planning of the multi-energy system based on the MINLP model was studied in [13], to address the optimal location and time of installation of multiple components in power and gas grids to minimize investment cost. In [14], a mixed-integer linear programming (MILP) model was developed for the optimal operation of integrated power and gas networks, considering line-pack capability with regard to steady-state and AC power flow models. In [15], a stochastic decentralized model for the operation and planning of interconnected gas and electricity networks was investigated. The real-time and short-term scheduling of the coordinated electricity and NG system in the presence of the power-to-gas facility and GF units was developed in [16]. The proposed model extends minute-scale gas flow, as well as the hourly scale power flow for the integrated system with the aim of operation cost minimization. Authors in [17] stated that GF units are an inseparable part of multi-carrier energy systems. The presence of these resources, coupled with electricity and gas networks, will pose several challenges. To address these challenges, the dynamic models for the NG grid have been investigated to better evaluate the interconnection of electrical and NG networks. The unit commitment model was extended in [18], including NG network and interdependency constraints between two systems aiming to minimize the operational cost. In [19], the resilience and vulnerability of interconnected electricity and NG networks in the micro-grid environment have been studied. To mitigate the negative effects of renewable energy fluctuations on the performance of multi-energy residential systems (MERS), the scheduling of these systems with regard to electricity and gas carriers has been proposed in [20].

The EH concept has attracted much attention for conversation, store, generation, and consumption of multiple energies. An interconnected EH model describes the transmission, conversion, and energy storage in a system, including several sub-regions [21]. All the challenges, weakness, and promising options of the EHs with a fast-growing toward multi-energy systems have been discussed by [22]. The authors of [23] stated that the interconnected EHs are a key factor in the multi-carrier system. Therefore, here, a multi-dimensional piecewise linear approximation approach was developed to simplify the complex NG transmission equation, as well as electrical power flow equation considering interconnected EHs. The energy management model of residential EH, including electricity and NG as inputs, was formulated based on the MILP model by [24]. The co-planning multi-EH system with NG and electrical carriers incorporated with high penetration of renewable energy based on the robust framework was evaluated by [25]. In [26], a new framework for optimal operation and planning of multi-energy systems considering EHs including CHP and GF units, was developed. The proposed framework determines the optimal capacity, location, and time of installation of new equipment over a 10-year period. The multi-energy network incorporating NG, heat and electricity networks based on distributed EHs was developed in [27]. In this study, the comprehensive model of integrated networks corresponding the restrictions based on the mixed-integer second-order cone programming was presented. In [28], a smart EH integrated with wind power and demand response to meet thermal and electrical loads considering energy prices uncertainty was developed. In [29], a novel EH system incorporated with CAES was developed for modelling transaction between power and heating networks using bi-level optimization framework.

Meanwhile, the flexible configuration for integrated energy system can provide extra benefits for utility and consumer from economic and technical perspectives. Reconfiguration

capability can be implemented at distribution level as a control option to reroute the power flows and maximize capacity utilization of the feeders, which in turn changes the GF unit commitment and gas flow in pipes. The authors in [30] stated that the future of the distribution networks will be envisaged as neighboring grids that exchange power through a reconfigurable framework. The bi-level optimization framework for reconfiguration of distribution networks to improve the system operation against any disaster events such as storm was investigated by [31] aiming at minimizing the load interruption cost. The risk-based optimal scheduling of reconfigurable microgrids integrated with wind energy based on the condition-value at risk (CVaR) criteria was evaluated in [32]. The proposed problem is formulated as a two-stage stochastic approach considering electricity price, wind power, and load demand variations. In [33], a novel heuristic method named switch opening and exchange approach has been implemented to solve a multi-hour network reconfiguration based on the stochastic framework. The authors of [34] have proposed a bi-level transactive energy trading framework to improve the energy dispatch of multi-carrier system, based on EH concept. The upper-level problem maximizes the social welfare of each EH, while the reconfiguration of the network is done by the system operator in the lower level to reduce the power loss. The optimal scheduling of the reconfigurable distribution network with considering the islanding capability based on the chance-constrained optimization model was extended by [35]aiming to minimize total operation cost.

However, the fast-growing installation of RESs with intermittent output, besides load and price uncertainties, results in optimal operation of multi-energy systems and it highlights the importance of risk management in such problems associated with random variables. The risk-averse stochastic programming of EH to serve both electrical and heat demands in the presence of the price uncertainty with the aim of operational cost minimization was developed by [36]. The risk-averse strategy in the security-constrained unit commitment model incorporated with battery storage system in the rail transportation was investigated by [37]. The proposed robust-stochastic approach analyzes the effects of battery-based rail transportation in the wind power curtailment reduction. The risk-based framework based CVaR was presented in [38] for optimal short-term energy and reserve operation of a virtual power plant integrated with wind energy and demand response.

1.3 | Research gaps and contributions of this work

Under the high interdependency between electricity and natural gas networks, it may be unrealistic and unreasonable if the two energy networks are operated separately. Thus, a comprehensive model of coordinated NG and reconfigurable electrical networks, considering all the limitations and interconnections between both gas and electrical grids, is urgently needed, which has rarely been studied in the literature. The remarkable gaps in the literature review can be outlined as follows:

- In [8–20], only the optimal operation of a coordinated energy system with a focus on security constraints of both networks has been studied, neglecting the reconfiguration capability and interconnected EHs.
- In [21–29], the authors focused on EHs scheduling as a basic infrastructure for the multi-carrier energy system, while security constraints and interdependency of gas and power grids have been ignored.
- In [30–35], although the reconfiguration capability of distribution networks has been investigated as a flexible solution, this capability for integrated gas and power grids has not been evaluated by each work.
- In [33–38], although the risk management in multiple problems has been studied, the risk-based optimal operation of integrated energy systems considering a comprehensive model for the interdependency of gas and power systems, and the reconfiguration capability under strong uncertainty has been ignored.

Based on the mentioned gaps, this paper concentrates on the risk-based optimal scheduling of integrated NG and reconfigurable electricity grids with distributed EHs. The proposed model is formulated as a two-stage stochastic approach considering the real-time power price, electrical load, and wind power variations. The distributed EHs equipped with CHP, gas boiler (GB), heat pump, and thermal storage are considered as connection points between NG and electricity distribution networks to supply both heating and electrical consumers. The AC-power flow and steady-state Weymouth gas flow equations are employed to model electrical and NG networks, respectively. Also, the risk-measure based on the conditional value-at-risk (CVaR) is extended to analyze the risk of the proposed model. The main contributions of this paper can be summarized as follows:

- Proposing a two-stage stochastic operation of coordinated NG and reconfigurable electricity networks. The proposed model considers all interactions between both carriers to reveal the effects of multiple technologies on the optimal daily scheduling.
- Implementing the AC-power flow and steady-state Weymouth equations for electricity and NG networks, respectively, under the reconfiguration capability for the first time to reveal the interdependence of both energy systems, achieving a more realistic model.
- Considering the interconnected EHs, containing multiple components beside gas-fired units as connection points between natural gas and electricity carriers under risk-based scheduling. The system operator can rely on the distributed EHs at different buses to supply local loads and reduce his dependency on the upstream gas and power market, results in the total operation cost reduction.
- Analyzing the consumption pattern of the gas-fired unit under hourly reconfiguration and its interactions with the gas network. The reconfiguration can affect the optimal power flow, and hourly unit commitment which results in gas flow changes in pipelines, consequently cost reduction.

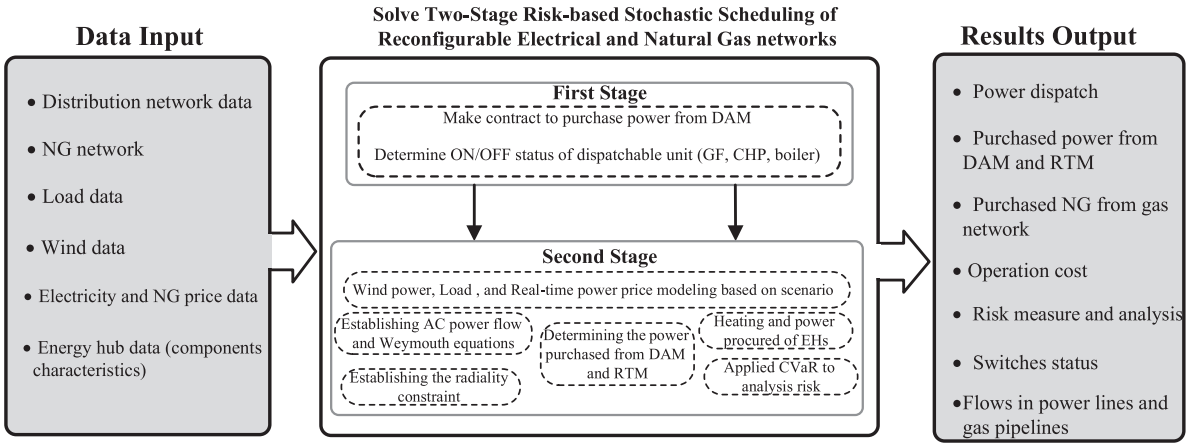

FIGURE 1 The schematic of proposed two-stage scheduling of coordinated electricity and NG networks

- Incorporating the risk-measure based on CVaR criteria in the MINLP model to evaluate the risk of expected cost considering load, wind energy, and energy price uncertainties on the decision making process by the integrated energy system's operator.

1.4 | Notation

The subscripts t and ω that were used for all variables in Nomenclature section demonstrate the amount of the variables at time t and scenario ω.

1.5 | Paper organization

The rest of this paper is organized in following order. Section 2 presents the problem description and formulation, including objective function and constraints related to both electrical and NG networks. The risk measure approach based on CVaR model is represented in Section 3. Section 4 contains the simulation and numerical results. Finally, Section 5 concludes the paper.

2 | PROBLEM FORMULATION

2.1 | Paper description

The optimal scheduling of coordinated electrical and NG networks considering reconfiguration capability and interconnected EHs (incorporated with CHP, GB unit, heat pump, and TES) is formulated as a two-stage stochastic model. The overall schematic of the proposed problem is depicted in Figure 1. The operator seeks to minimize the operational cost of coordinated NG electrical systems, considering a load demand, wind energy and real-time power price variability. The power purchased from the day-ahead market (DAM), and unit commitment are determined at the first stage as here-and-now variables. Based on wind power, load and real-time power price uncertainty modelling using the scenario-based stochastic framework, the optimal power dispatch, purchasing NG and electricity from gas market and real-time market (RTM), respectively, and energy procured by each interconnected EHs are determined as wait-and-see variables in the second stage. It should be noted that the electricity and thermal procedure of each EH has a significant effect on the GF units, as well as power and gas purchased from the markets. The risk-measure based on CVaR criteria is implemented by the operator to mitigate the risk of expected cost based on the optimal solution for power dispatch of GF units, energy procured of interconnected EHs, hourly switches status, and power and NG exchanged with corresponding markets based on AC-power flow and steady state Weymouth models.

2.2 | Objective function

The objective function of the proposed model is represented by (1). The first term of (1) denotes the purchased power cost from the DAM. The start-up and shut-down cost related to the GF and CHP units are represented by second and third terms of (1), respectively. The cost of purchased power from the RTM is expressed by fourth term of (1). The generation cost of GF by fifth term of (1). The cost of purchased NG from the gas market is given in sixth term of (1). Finally, the switching cost for any switching action as [35], is represented by seventh term of (1).

$$\begin{aligned} \textit{Min}\ \mathrm{OF} = \sum_{t=1}^{NT} \Bigg[& \lambda_t^D EM_t + \left(\sum_{g=1}^{NU} SU_{g,t} + SD_{g,t} \right) \\ & + \left(\sum_{n=1}^{NC} SU_{n,t} + SD_{n,t} \right) + \sum_{\omega=1}^{NS} \pi_\omega \\ & \left[\lambda_{t,\omega}^R RM_{t,\omega} + \sum_{g=1}^{NG} F\left(P_{g,t,\omega}\right) \right. \\ & \left. + \lambda_t^G GM_{t,\omega} + \sum_k C^{sw} N_{k,t,\omega}^{sw} \right] \Bigg]. \end{aligned} \tag{1}$$

2.3 | Problem constraints

The proposed scheduling of coordinated reconfigurable electrical and NG networks is restricted by multiple constraints as follows.

- Gas-fired unit constraints

The fast-growing installation of GF units makes the electricity sector as an important player in the gas industry, which has led to a strong interaction between electricity and NG networks. The operation of GF units is limited by different constraints such as active and reactive power output, ramp-up/ ramp-down, minimum up/down times, and etc., which are provided by [3].

- Electrical energy storage constraints

This study shows battery energy storage system (BESS) is embedded in the power system to facilitate the integration of wind energy and preserve load balance. The BESS charging and discharging power are bounded by upper and lower values, as represented in (2) and (3), respectively. The binary variables to separate the charging and discharging modes at each time is established in (4). If BESS operates in charging mode, $x^{ch}_{b,t,\omega} = 1$ and constraint (3) is imposed, being 0 otherwise, and constraint (2) is imposed. Constraints (5)–(7) are related to energy capacity and state-of-charge (SOC) of BESS.

$$P^{dis,\min}_{b} x^{dis}_{b,t,\omega} \le P^{dis}_{b,t,\omega} \le P^{dis,\max}_{b} x^{dis}_{b,t,\omega}, \tag{2}$$

$$P^{ch,\min}_{b} x^{ch}_{b,t,\omega} \le P^{ch}_{b,t,\omega} \le P^{ch,\max}_{b} x^{ch}_{b,t,\omega}, \tag{3}$$

$$x^{ch}_{b,t,\omega} + x^{dis}_{b,t,\omega} \le 1, \tag{4}$$

$$SOC_{b,t+1,\omega} = SOC_{b,t,\omega} + \eta^{ch}_{b} P^{ch}_{b,t,\omega} - \frac{P^{dis}_{b,t,\omega}}{\eta^{dis}_{b}}, \tag{5}$$

$$SOC_{b,t=24,\omega} = SOC_{b,int}, \tag{6}$$

$$SOC^{\min}_{b} \le SOC_{b,t,\omega} \le SOC^{\max}_{b}. \tag{7}$$

- Power flow and radiality constraints

The active and reactive power balance between supply and demand sides at each bus and other power flow limits are established by (8)–(17). The active and reactive power balance are established by (8) and (9), respectively. It should be noted that the first two terms in (8) and (9) must be eliminated for each bus except for slack bus (main bus that make the connection between electrical system and upstream network). Also, the third term in (8) and (9) are related to the active and reactive power of EH which are considered for buses with EHs (buses with i' index). The active and reactive power flow in the distribution feeder considering the reconfiguration capability are represented by (10) and (11). The amount of power exchanged with the upstream network is limited by (12) [39]. The thermal capacity of feeder is established by (13). Constraint (14) shows the voltage limit for each bus. However, the radiality structure of distribution network should be maintained; hence the optimal structure should not contain any loop at each time. To establish the radiality constraint, the number of open switches pre and after reconfiguration must be equaled as (15). It should be noted that the possible loops in the distribution network structure are found only once after equipment installation. To prevent making any loop in distribution network structure, constraint (16) is imposed. Also, the number of total switching action to calculate the switching cost term is determined by (17).

$$\begin{aligned} &EM_t + RM_{t,\omega} + \sum_{b\in H_{i'}} P^{hub}_{b,t,\omega} + \sum_{g\in G_i} P_{g,t,\omega} + P_{wi,t,\omega} \\ &\quad + \sum_{b\in B_i} \left(P^{dis}_{b,t,\omega} - P^{ch}_{b,t,\omega}\right) - \sum_{d\in D_i} P_{d,t,\omega} \\ &= \sum_{j\in J_i} PF_{ij,t,\omega}, \end{aligned} \tag{8}$$

$$\begin{aligned} &QEM_t + QRM_{t,\omega} + \sum_{b\in H_{i'}} Q^{hub}_{b,t,\omega} + \sum_{g\in G_i} Q_{g,t,\omega} \\ &\quad + Q_{wi,t,\omega} - \sum_{d\in D_i} Q_{d,t,\omega} = \sum_{j\in J_i} QF_{ij,t,\omega}, \end{aligned} \tag{9}$$

$$\begin{aligned} PF_{ij,t} = \big[&V_{i,t,\omega} V_{j,t,\omega} \big(G_{ij} \cos(\delta_{i,t,\omega} - \delta_{j,t,\omega}) \\ &+ B_{ij} \sin(\delta_{i,t,\omega} - \delta_{j,t,\omega})\big)\big] K_{ij,t,\omega}, \end{aligned} \tag{10}$$

$$\begin{aligned} QF_{ij,t} = \big[&V_{i,t,\omega} V_{j,t,\omega} \big(G_{ij} \sin(\delta_{i,t,\omega} - \delta_{j,t,\omega}) \\ &- B_{ij} \cos(\delta_{i,t,\omega} - \delta_{j,t,\omega})\big)\big] K_{ij,t,\omega}, \end{aligned} \tag{11}$$

$$\left(EM_t + RM_{t,\omega}\right)^2 + \left(QEM_t + QRM_{t,\omega}\right)^2 \le S^2_{up}, \tag{12}$$

$$PF^2_{ij,t,\omega} + QF^2_{ij,t,\omega} \le (S^{\max}_{ij})^2, \tag{13}$$

$$V^{\min}_{i} \le V_{i,t,\omega} \le V^{\max}_{i}, \tag{14}$$

$$\sum_{i,j\in NI}^{NLI_{LP}} K_{ij,t,\omega} = NLI_{IS}, \tag{15}$$

$$\sum_{i,j\in NI}^{NLI_{LP}} K_{ij,t,\omega} \le NLI_{LP} - 1, \tag{16}$$

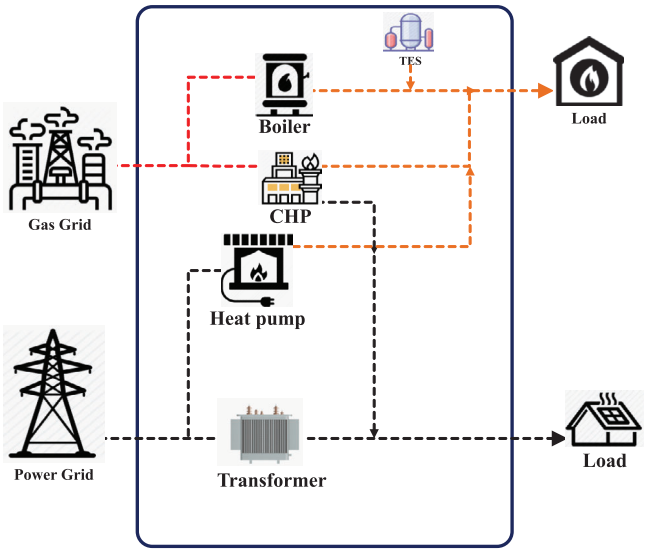

FIGURE 2 Structure of interconnected energy hub model

$$N^{sw}_{k,t,\omega} = \sum_{t}^{NLI_{I,P}} \left| \left(K_{ij,t,\omega} - K_{ij,t-1,\omega} \right) \right| . \tag{17}$$

- EH constraints

The interconnected EH is considered to be the connection point between electricity and NG networks as well as bidirectional connection at coupling points with energy networks. The proposed EH model is shown in Figure 2.

The proposed EH can contain the GB, CHP, heat storage, transformer and electrical pump. The operation of EH is restricted by multiple limitations described as follows.

- Energy balance constraints (power and heat balance)

Constraints (18) and (19) demonstrate the active and reactive power balance in the interconnected EH. The right term of constraint (18) denotes the power exchanged between the hub and the corresponding bus. In other words, the EH can be back into the bus. The thermal balance limit is represented by (20).

$$\sum_{n\in N_i} P_{n,t,\omega} - \sum_{tr\in TR_i} P^{tr}_{t,\omega} - \sum_{hp\in Hp_i} P^{hp}_{t,\omega} - \sum_{d\in D_i} P^{hub}_{d,t,\omega} = P^{hub}_{h,t,\omega}, \tag{18}$$

$$\sum_{n\in N_i} Q^{chp}_{n,t,\omega} - \sum_{tr\in TR_i} Q^{tr}_{t,\omega} - \sum_{hp\in Hp_i} Q^{hp}_{t,\omega} - \sum_{d\in D_i} Q_{d,t,\omega} = 0, \tag{19}$$

$$\sum_{n\in N_i} H^{chp}_{n,t,\omega} + \sum_{bo\in Bo_i} H^{bo}_{t,\omega} + \sum_{hp\in Hp_i} \alpha^{hp} P^{hp}_{t,\omega} + \sum_{hs\in Hs_i} \left(H^{hs,dis}_{t,\omega} - H^{hs,ch}_{t,\omega} \right) = \sum_{d\in D_i} H_{d,t,\omega} . \tag{20}$$

- GB constraints

Constraint (21) represents the limitation of produced heat by GB unit which is bounded by maximum and minimum values. The fuel function of GB represents the consumed NG by it that is expressed by (22), where HR^{bo} is heat rate for the GB.

$$H^{bo,\min} \varkappa^{bo}_{t} \le H^{bo}_{t,\omega} \le H^{bo,\max} \varkappa^{bo}_{t}, \tag{21}$$

$$GB^{bo}_{t,\omega} = HR^{bo} H^{bo}_{t,\omega}. \tag{22}$$

- TES constraints

The thermal energy storage (TES) facility is coupled with GB and CHP unit to provide more flexibility in thermal load supply. Similar to BESS, TES can only operate either in charging or discharging mode, established by (23). The charge and discharge value limits are represented by (24) and (25), respectively. Constraint (26) represents the current thermal energy content of TES. This value is limited by the maximum value as established in (27). Constraint (28) imposes equality condition for TES.

$$I^{hs,dis}_{t,\omega} + I^{hs,ch}_{t,\omega} \le 1, \tag{23}$$

$$H^{hs,dis,\min} I^{hs,dis}_{t,\omega} \le H^{hs,dis}_{t,\omega} \le H^{hs,dis,\max} I^{hs,dis}_{t,\omega}, \tag{24}$$

$$H^{hs,ch,\min} I^{hs,ch}_{t,\omega} \le H^{hs,ch}_{t,\omega} \le H^{hs,ch,\max} I^{hs,ch}_{t,\omega}, \tag{25}$$

$$HS^{hs}_{t,\omega} = HS^{hs}_{t-1,\omega} + eh^{ch} H^{hs,ch}_{t,\omega} - \frac{H^{hs,dis}_{t,\omega}}{eh^{dis}}, \tag{26}$$

$$HS^{hs,\min} \le HS^{hs}_{t,\omega} \le HS^{hs,\max}, \tag{27}$$

$$HS_{t=0} = HS_{t=24}. \tag{28}$$

- Heat pump and transformer constraints

Heat pumps transfer thermal energy in the opposite direction of spontaneous heat transfer. The active and reactive power consumption by heat pump are bounded by minimum and maximum values, as represented by (29) and (30), respectively.

As the heat pump, there are active and reactive power limits on the transformer operation which are bounded by the minimum and maximum values as [40].

$$0 \le P_{t,\omega}^{hp} \le P^{hp,\max}, \tag{29}$$

$$0 \le Q_{t,\omega}^{hp} \le Q^{hp,\max}. \tag{30}$$

- CHP unit constraints

Generally, the produced heat and power by CHP unit depend to each other. The produced power (active and reactive power outputs) and heat limits b CHP unit are given by (31)–(33). HPR_n and η^{be} are, respectively, heat to power and heat exchange efficiency [28]. The generated power by CHP cannot change rapidly. Therefore, the ramp-up and ramp-down constraints for CHP should be established as (34) and (35), respectively. The start-up and shut-down costs related to the CHP are represented in (36)–(39).

$$P_n^{\min} u_{n,t} \le P_{n,t,\omega} \le P_n^{\max} u_{n,t}, \tag{31}$$

$$Q_n^{\min} u_{n,t} \le Q_{n,t,\omega} \le Q_n^{\max} u_{n,t}, \tag{32}$$

$$H_{n,t,\omega} \le P_{n,t,\omega} \times HPR_n \times \eta^{be}, \tag{33}$$

$$P_{n,t,\omega} - P_{n,t-1,\omega} \le R_n^{up}, \tag{34}$$

$$P_{n,t-1,\omega} - P_{n,t,\omega} \le R_n^{dn}, \tag{35}$$

$$SU_{n,t} \ge SUC_n(u_{n,t} - u_{n,t-1}) \tag{36}$$

$$SU_{n,t} \ge 0 \tag{37}$$

$$SD_{n,t} \ge SDC_n(u_{n,t-1} - u_{n,t}), \tag{38}$$

$$SD_{n,t} \ge 0. \tag{39}$$

- Natural gas network constraints

Equation (40) models the gas flow in a pipeline as a non-linear function of pipeline characteristics and node pressure. The sgn is the sign function as formulated in (41). The amount of gas flow in pipeline is limited by maximum value as (42). The pressure of gas node is limited by the minimum and maximum values as given by (43). As electrical network, the gas balance should be established at each gas node. Therefore, constraint (44) represents the gas balance between production and consumption sides, where $G_{d,t,\omega}$ is the gas loads, including GF units and EH's input described in the following. The scheduled value of the purchased NG from the gas market is calculated by (45), while the gross heating value is applied to convert the volume of the NG to the energy value [41]. This value is limited by constraint (46).

$$G_{lm,t,\omega}^{line} = sgn\left(\rho_{l,t,\omega}, \rho_{m,t,\omega}\right) C_{lm} \sqrt{\left|\left(\rho_{l,t,\omega}^2 - \rho_{m,t,\omega}^2\right)\right|}, \tag{40}$$

$$sgn\left(\rho_{l,t,\omega}, \rho_{m,t,\omega}\right) = \begin{cases} +1 & \text{if} \quad \rho_{l,t,\omega} - \rho_{m,t,\omega} > 0 \\ -1 & \text{if} \quad \rho_{l,t,\omega} - \rho_{m,t,\omega} < 0, \end{cases} \tag{41}$$

$$\left|G_{lm,t,\omega}^{line}\right| \le G_{lm}^{line,\max}, \tag{42}$$

$$\rho_l^{\min} \le \rho_{l,t,\omega} \le \rho_l^{\max}, \tag{43}$$

$$GM_{t,\omega} - \sum_{d \in D_l} G_{d,t,\omega} = \sum_{m \in M_l} G_{lm,t,\omega}^{line}, \tag{44}$$

$$GM_{t,\omega} = GHV \times \sum_{d \in D_t} G_{d,t,\omega}, \tag{45}$$

$$0 \le GM_{t,\omega} \le GM^{\max}. \tag{46}$$

- Electrical and NG coupling constraints

The GF units and interconnection EHs are the two gas consumers, which make connection points between electrical and NG networks. As [9], the gas consumption by GF unit is modelled based on the quadratic function. Also, the gas balance and maximum gas consumption by GF unit and EH are bounded by the maximum values, which are represented in [9].

3 | RISK MANAGEMENT

3.1 | Risk measure based on CVaR

In optimization problems associated with multiple uncertainties, including RES fluctuation, load demand, as well as energy prices, the objective function can be specified by the stochastic programming criteria such as expected value. The expected value of the objective function is the most useful criterion that is applied in such stochastic programming problems. Despite the

multiple advantages of utilization of the expected value criterion for the problem associated with random variables, the main impediment of this approach is that it only shows an average of multiple scenarios [41] and [42]. In other words, the optimal value of the objective function in some scenarios may be far from the average value, while more acceptable to the decision-maker. Therefore, control of the risk of experiencing cost in the presence of different random variables is essential. CVaR with unique features can assess and manage the risk associated with wind energy, load demand, and electricity price in the RTM. The general form of CVaR can be formulated as follows:

$$\xi + \frac{1}{1-\alpha}\sum_{\omega=1}^{NS}\pi_{\omega} \times s_{\omega}, \tag{47}$$

$$OF_s - \xi \leq s_{\omega}, \tag{48}$$

$$s_{\omega} \geq 0, \tag{49}$$

where α is confidence level, ξ is value at risk, s_{ω} is non-negative and continuous variables which equals to the maximum value of $OF_s - \xi$, and equals to 0, if the value of the left side of (48) is negative. It should be noted that the confidence level (α) is considered to be 0.95 and β has been increased from 0 to 1 in fixed steps.

3.2 | CVaR-based optimal scheduling of coordinated electrical and NG distribution systems

The risk-constrained scheduling of coordinated NG and reconfigurable electricity distribution networks incorporated with interconnected EHs with multiple terms in the objective function (1) can be reformulated based on the risk measure strategy which was described in previous section as follows:

$$\begin{aligned} Min\text{OF} =& (1-\beta)\times \\ & \sum_{t}\left[\lambda_t^D EM_t + \left(\sum_{g=1}^{NU} SU_{g,t} + SD_{g,t}\right) + \left(\sum_{n=1}^{NC} SU_{n,t} + SD_{n,t}\right)\right. \\ & \left. + \sum_{\omega=1}^{NS}\pi_{\omega}\left[\lambda_{t,\omega}^R RM_{t,\omega} + \sum_{g=1}^{NG} F_c\left(P_{g,t,\omega}\right) + \lambda_t^G GM_{t,\omega}\right.\right. \\ & \left.\left. + \sum_{k} C^{sw} N_{k,t,\omega}^{sw}\right]\right] \\ & -\beta\left(\xi + \frac{1}{1-\alpha}\sum_{\omega=1}^{NS}\pi_{\omega} \times s_{\omega}\right), \end{aligned} \tag{50}$$

where $\beta \in 0,1$ is a risk parameter that is used to specify the compromise between cost function and risk aversion. The proposed CVaR-based objective function (50) is subjected to following constraints:

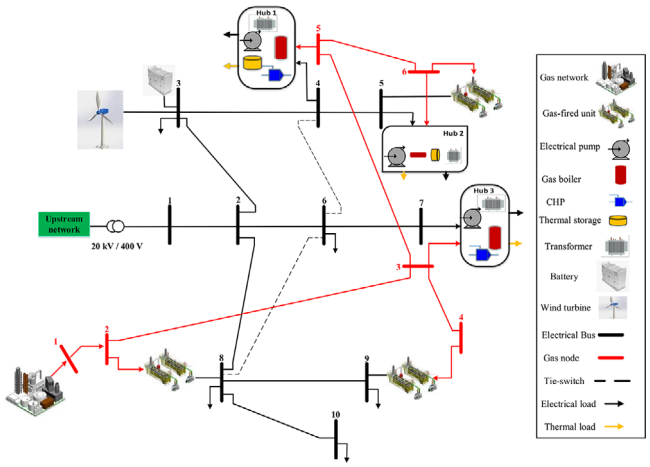

FIGURE 3 Structure of integrated NG and reconfigurable electrical networks

$$\left\{\begin{aligned} & \lambda_t^D EM_t + \left(\sum_{g=1}^{NU} SU_{g,t} + SD_{g,t}\right) \\ & + \left(\sum_{n=1}^{NC} SU_{n,t} + SD_{n,t}\right) + \lambda_{t,\omega}^R RM_{t,\omega} \\ & + \sum_{g=1}^{NG} F\left(P_{g,t,\omega}\right) + \lambda_t^G GM_{t,\omega} + \sum_{k} C^{sw} N_{k,t,\omega}^{sw} \end{aligned}\right\} - \xi \leq s_{\omega} \tag{51}$$

$$t \in NT,$$

$$s_{\omega} \geq 0, \tag{52}$$

$$(2) - (46). \tag{53}$$

4 | SIMULATION RESULTS

4.1 | Case study

The integrated distribution energy system including reconfigurable electrical and NG networks test case as shown in Figure 3 was utilized to verify the effectiveness of the proposed risk-based optimal scheduling. A modified 10-bus reconfigurable distribution network, including two tie-switches and nine sectionalizing lines, and three gas-fired units (at bus 5, 7, and 8) are implemented. All characteristics of 10-bus distribution system are presented in [32]. The 500 kW wind turbine is included in distribution system, which is located in bus 3. Also, the battery energy storage is located in bus 3, with 50 kW maximum charging and discharging and 200 kWh capacity.

TABLE 1 Existing components in each EH

Hub	CHP	GB	Heat pump	TES
1	✓	✓	✓	✓
2	×	✓	✓	✓
3	✓	✓	✓	×

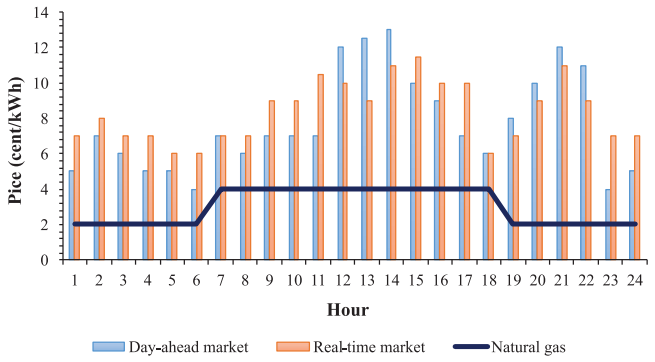

FIGURE 4 The hourly energy price

Also, a modified 6-nodes natural gas network is used in this paper [41]. The maximum allowable NG volume pass from the main pipeline is 420 cubic meter per hour. The three NG-fired units are supplied from nodes 1, 3, and 5. The minimum and maximum limits of NG pipeline pressure are 0.2 and 1.3 (p.u.), respectively.

There are three interconnected EHs in the multi-energy system, which are located in buses 4, 5 and 7 and nodes 4, 5 and 2, respectively. The existing resources in each EH is shown in Table 1. Also, characteristics of embedded resources in EHs are given in [41]. The electrical and thermal loads of 3 interconnected EHs are given in [40].

Figure 4 shows the real-time price, NG price as well as day-ahead power price. The mean value of electrical load (active and reactive), and wind energy scenarios are shown in Figure 5.

It should be noted that all uncertain parameters are subjected to the corresponding probability distribution function with unique features. More information can be found in [43].

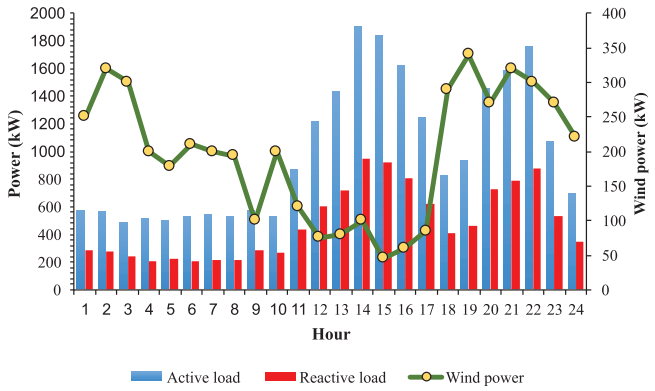

FIGURE 5 The hourly load demand and wind energy

TABLE 2 Total operation cost and corresponding probability for 10 reduction scenarios in Case 1 and 2

Scenario	Cost for Case 1 ($)	Cost for Case 2 ($)	Probability
1	2414.632	2360.885	0.0602
2	2357.841	2406.126	0.1402
3	2279.633	2396.551	0.1322
4	2498.254	2510.612	0.1076
5	2674.340	2516.780	0.1376
6	2759.441	2543.671	0.1333
7	2598.674	2347.256	0.1991
8	2601.940	2478.632	0.0352
9	2500.687	2390.145	0.0225
10	2467.493	2407.677	0.0321
Expected cost($)	2520.771	2435.833	

4.2 | Numerical results

The proposed risk-constrained scheduling of coordinated NG and reconfigurable electrical distribution systems incorporated with distributed EHs, considering AC power flow and Weymouth equations was formulated as MINLP model, carried out in GAMS software and solved with SBB solver. The simulation results are provided for the following cases:

- Case 1: Optimal scheduling of coordinated natural gas and electrical distribution networks without reconfiguration capability.
- Case 2: Case 1 considering reconfiguration capability.
- Case 3: CVaR-based scheduling for Case 2.

In order to capture the benefit of reconfiguration capability, numerical results for two first cases are presented, simultaneously, which facilitates the comparison between the obtained results. Table 2 presents total operation cost in 10 scenarios for Case 1 and Case 2 with corresponding probabilities. Also, the expected operation cost in Case 1 and Case 2 is given in this table. The reconfiguration capability in Case 2 reduces the expected operation cost by 7.82%, with respect to Case 1. For more explanations, scenario number 6 with the most expensive total operational cost (worst case scenario) is selected and is provided in detail.

Figure 6 depicts the power dispatch in scenario number 6. According to Figure 6, in Case 2, GF 1 as a high-cost unit is committed few hours in comparison with Case 1 (only peak hours: 13–16 and 21–22). Also, at lower electricity price (1–7), by adjusting the switches status and using the maximum feeders' capacity through reconfiguration, the system operator tends to purchase more power from DAM and RTM, instead of turning on the GF2 in Case 2. Furthermore, the battery energy storage has the same behaviour, in comparison with Case 1, due to the purchasing of more power from both markets, the battery is charged more in Case 2, and injects the power to the system at peak hours.

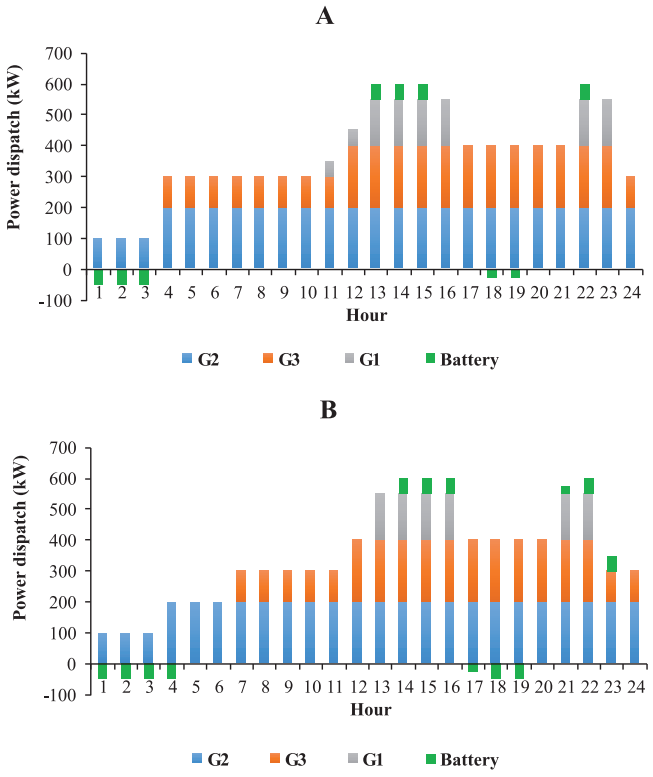

FIGURE 6 Hourly optimal power dispatch of GF units and battery: (a) Case 1; (b) Case 2

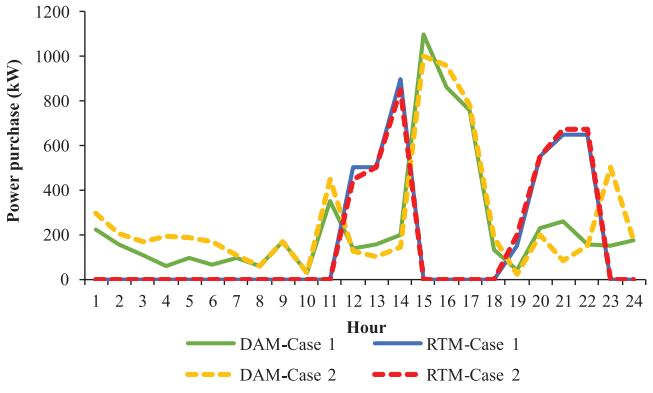

FIGURE 7 Hourly power purchased from DAM and RTM for Case 1 and Case 2

Figure 7 shows the power purchased from DAM and RTM in Case 1 and Case 2, for scenario number 6. According to Figure 4, for the time period including 1–11, 15–18, and 23–24, the DAM prices is less than RTM prices and it is economical for the operator to purchase more power from the DAM as depicted in Figure 7. As can be seen from this figure, in comparison with Case 1, the reconfiguration capability enables the operator to purchase more power from DAM in Case 2. The main reason for this phenomenon is that the reconfiguration transfers the electrical load from heavily loaded parts to lightly ones contributing to more economic benefits. In other words, using the reconfiguration to improve the power loss and adjust

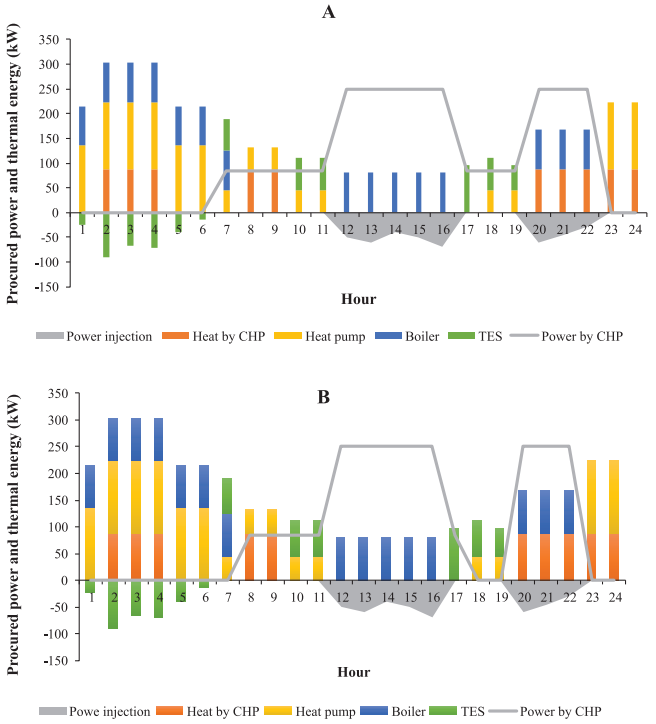

FIGURE 8 The procured power and thermal energy for EH1: (a) Case 1; (b) Case 2

the switches status, enables the operator to purchase more electricity at lower prices (1–7) and contributes to more economic savings from the electricity supply side. The opposite of this procedure is true for higher prices (13–16, and 20–22). Also, the power purchased from the RTM is increased at this period, due to declining RTM in comparison with DAM for both cases.

The procured electrical and thermal energy for three interconnected EHs in scenario number 6 are analyzed separately.

- Energy Hub 1

Figure 8 shows the procured electrical and thermal energy of EH 1. For the time period with lower electricity prices (1–7 and 23–24), more power injects to EH 1. In this period, the heat pump operates with the maximum capacity to supply thermal loads. In both cases, for lower electricity prices, more power is injected into EH 1, consequently, the injected NG is reduced. In contrast, for the time periods with higher prices, more NG is injected, and the power injection is reduced. The main reason for this phenomenon is that the main part of the injected NG is burned by the CHP to generate electricity with the maximum capacity, and supply electrical load at peak hours. Furthermore, according to Figure 8, in the time periods 12–16 and 20–22, the extra power generated by the CHP back into the bus, when the electricity price reaches higher values and contributes to more economic saving by the operator. The optimal scheduling of the GB and TES are also following the thermal demand. The only noticeable difference between the two cases is the increase in power injection in lower electricity prices and

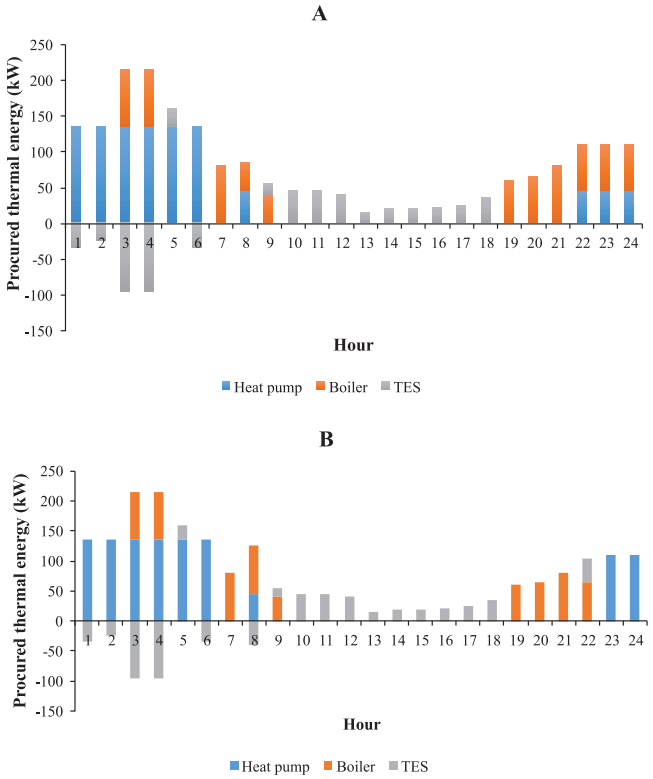

FIGURE 9 The procured power and thermal energy for EH2: (a) Case 1; (b) Case 2

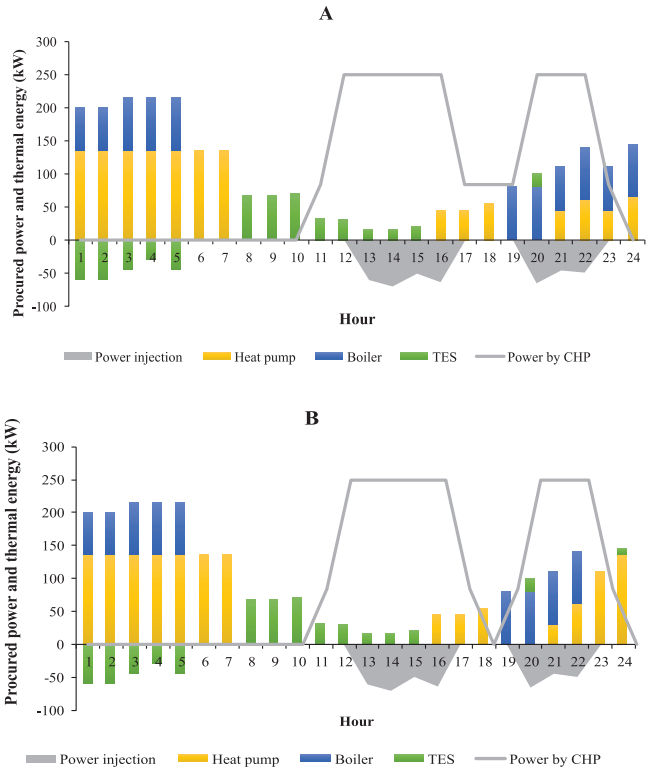

FIGURE 10 The procured power and thermal energy for EH3: (a) Case 1; (b) Case 2

consequent decrease in gas injection due to the reconfiguration capability.

- Energy Hub 2

Figure 9 shows the procured electrical and thermal energy for EH2 in Case 1 and Case 2. The EH 2 has a higher thermal loads and the CHP unit is not embedded. For the time period with lower electricity prices, the heat pump operates with the maximum capacity in both cases. The GB operates with the maximum capacity to supply thermal loads. In comparison with EH1, TES discharges more hours. At the initial time of day, TES is charged by the generated heat from the heat pump and GB and injects the stored heat when the gas price is higher or pump heat is off. The power injection in Case 2 is more than Case 1 thanks to the reconfiguration capability. For example, at 18 and 23–24 (lower electricity prices), more power injected to turn on the heat pump, in comparison with Case 1.

- Energy Hub 3

The procured electrical and thermal energy for EH3 is depicted in Figure 10. For time periods with lower electricity prices, more power is injected to EH3 in both cases. Although reconfiguration capability causes more power injection from the corresponding bus in Case 2, in comparison with Case 1 (for example at 23–24). The EH3 has more electrical load and relatively less thermal demand. Therefore, the CHP unit is used only for electricity supply and the heat generated by the CHP is zero. Also, at 13–16, the extra power generated by CHP back into the network. The optimal scheme of the GB and TES also follow the thermal demand to minimize operation cost through the reduction of the NG consumption.

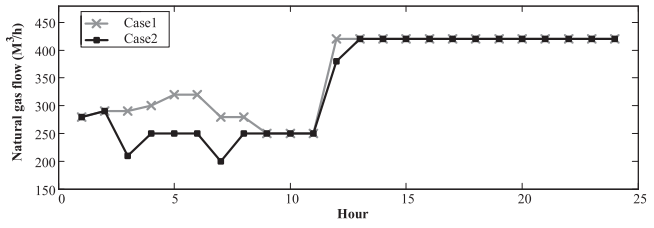

FIGURE 11 The hourly natural gas flow rate in main pipeline for Case 1 and Case 2

The optimal switches status in Case 2 for scenario number 6 is given by Table 3. At each time, two switches are opened to establish the radiality constraint. Using the reconfiguration to improve the power loss and adjust the switches status causes the maximum utilization of feeder capacity and consequent reduction of operation cost.

Figure 11 shows the NG flow in the main pipeline between the gas grid and system to supply gas loads, including three interconnected EHs, and three GF units for both cases in scenario 6. As previously discussed, the local gas consumers' supply via EHs have more priority than GF units. The effect of

TABLE 3 The hourly optimal structure of distribution network in Case 2

Hour	Close switches	Open switches
1	1,2,3,4,5,6,7,8,9	10,11
2	1,3,4,5,6,7,8,9,10	2, 11
3	1,3,4,5,6,7,8,9,10	2, 11
4	1,3,4,5,6,7,8,9,10	2, 11
5	1,3,4,5,6,7,8,9,10	2, 11
6	1,3,4,5,6,7,8,9,10	2, 11
7	1,3,4,5,6,7,8,9,10	2, 11
8	1,3,4,5,6,7,8,9,10	2, 11
9	1,2,3,4,5,6,7,8,9	10,11
10	1,2,3,4,5,6,7,8,9	10,11
11	1,2,3,4,5,6,7,8,9	10,11
12	1,2,3,4,5,6,7,8,9	10,11
13	1,2,3,4,5,6,7,8,9	10,11
14	1,2,3,4,5,6,7,8,9	10,11
15	1,3,4,5,6,8,9,10,11	2, 7
16	1,3,4,5,6,8,9,10,11	2, 7
17	1,3,4,5,6,7,8,9,10	2, 11
18	1,3,4,5,6,8,9,10,11	2, 7
19	1,2,3,4,5,6,8,9,11	7, 10
20	1,3,4,5,6,8,9,10,11	2, 7
21	1,3,4,5,6,8,9,10,11	2, 7
22	1,2,3,4,5,6,8,9,11	7, 10
23	1,2,3,4,5,6,8,9,11	7, 10
24	1,3,4,5,6,7,8,9,10	2, 11

the reconfiguration capability on the burned NG by the GF units and EHs is quite obvious. Reconfiguration by using the maximum feeder capacity can change the power dispatch, and consequently gas flow. As presented in results, for the time periods with lower electricity prices, more power injected from the DAM and RTM and GF units' behaviour are completely changed. This action results in the gas consumed by the integrated system. According to Figure 11, at 1–7, the NG flow is reduced in Case 2. The main reason for this phenomenon is that the G3 is less committed, and the thermal loads are supplied via a heat pump, therefore, less NG burned.

- **Case 3**

In the following, the risk management of the proposed scheduling problem is evaluated. The effects of risk parameter (β) on the values of multiple variables are analyzed. The values of β depending on the operator's performance in the face of risk management. The risk-taker operator prefers the values of β to reach a fewer operation cost with high risk, while the risk-averse operator prefers values of β to reduce the risk.

Figure 12 depicts the values of CVaR per the expected cost for different values of β. According to this figure, the high expected operation cost is obtained at low risk, while at high

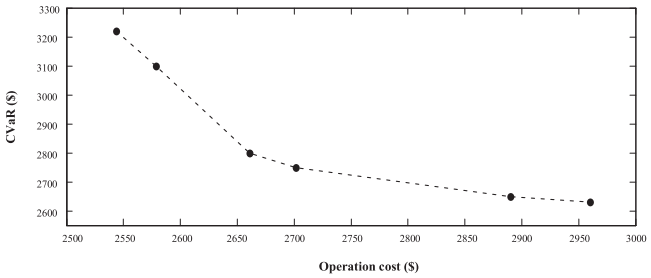

FIGURE 12 Variation of CVaR and operation cost for different values of β

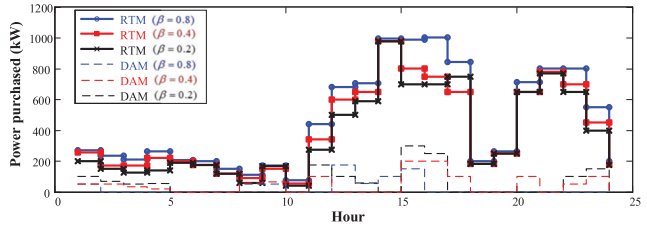

FIGURE 13 Power purchased from real-time and day-ahead markets for different values of β

risk level the expected cost is reduced. Also, by increasing β, CVaR is reduced.

The power purchased from day-ahead and real-time markets for three different values of β is shown in Figure 13. By increasing β, the power purchased from DAM is increased, while the power purchased from RTM reduces. This action is caused by the risk associated with real-time electricity prices.

The optimal daily structure including opened switches for different values of β is given by Table 4. According to Table 4, changing β results in an optimal hourly topology.

The NG flow rate in the pipeline between main pipeline and the system for different values of β is shown by Figure 14. By increasing β, for the time period between 7–24, the NG flow is reduced compared with Case 2 ($\beta = 0$). The main reason for this phenomenon is the significant increase of power purchased from the DAM. Therefore, the risk-taker operator trends to purchase more electricity and minimize the NG purchased for the operation cost reduction, based on NG price conditions (depicted in Figure 4).

Here, the reconfiguration process is considered in the optimal scheduling of coordinated gas and power distribution systems. As discussed in the radiality constraint, the offline method is employed to find the possible loop in the structure. After that, the number of open and closed switches at each period according to (15) and (16) is calculated, without any complication in the radiality modelling compared to the branch incidence matrix. However, there are different solutions in the literature to solve the reconfiguration problem like the heuristic method. Genetic algorithm (GA) and particle swarm optimization (PSO) are the two most known heuristic approaches which have been mainly implemented in several problems in the power system operation. To reveal the effectiveness of the proposed model for the integrated gas and reconfigurable electrical

TABLE 4 The optimal hourly opened switches for different values of β

Hour	$\beta = 0.2$	$\beta = 0.4$	$\beta = 0.8$
1	7, 10	10,11	2, 11
2	7, 10	2, 11	2, 11
3	7, 10	2, 11	2, 11
4	5, 11	2, 11	2, 7
5	5, 11	2, 11	2, 7
6	5, 11	2, 11	2, 7
7	5, 11	2, 11	2, 7
8	5, 11	2, 11	2, 7
9	4, 5	10, 11	10, 11
10	4, 5	10,11	10, 11
11	4, 5	10,11	10, 11
12	10, 11	10,11	10, 11
13	10, 11	10,11	10, 11
14	10, 11	10,11	10, 11
15	2, 7	10,11	2, 11
16	2, 7	2, 7	10, 11
17	2, 7	2, 7	10, 11
18	2, 7	2, 11	2, 11
19	2, 11	7, 10	2, 11
20	2, 11	2, 11	2, 11
21	10, 11	2, 7	10, 11
22	7, 10	7, 10	10, 11
23	7, 10	7, 10	10, 11
24	7, 10	2, 11	2, 11

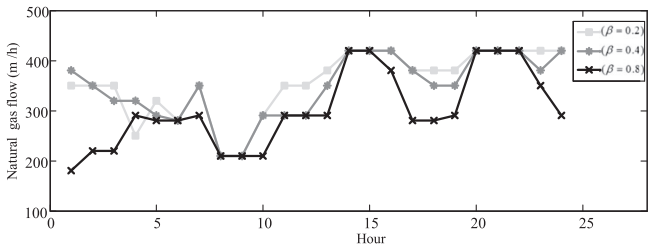

FIGURE 14 Variation of natural gas flow in main pipeline for different values of β

distribution network, we compared the major conclusion obtained from the reconfiguration results with GA and PSO as represented in Table 5. These methods act based on the fitness function and a large number of iterations are required for converging. To find the optimal topology, both algorithms establish the radiality constraint based on the branch incidence matrix. As shown in Table 5, the proposed model has much less execution time compared to the GA and PSO. In terms of obtained topology at each hour, there is no noticeable difference between the results. Furthermore, the expected operation cost examined by the proposed model is 12.5% and 14.7% less than the GA and PSO methods, respectively.

TABLE 5 The comparison of the proposed method with similar techniques from run time, operation cost, and hourly topology

Hour	GA	PSO	Proposed method
1	2, 11	2,11	10, 11
2	2, 11	2, 11	2, 11
3	2, 11	2, 11	2, 11
4	2, 11	2, 11	2, 11
5	2, 11	2, 11	2, 11
6	2, 11	2, 11	2, 11
7	2, 11	2, 11	2, 11
8	2, 11	2, 11	2, 11
9	2, 11	10, 11	10, 11
10	2, 11	10,11	10, 11
11	2, 11	10,11	10, 11
12	10, 11	10,11	10, 11
13	10, 11	10,11	10, 11
14	10, 11	10,11	10, 11
15	10, 11	10,11	2, 7
16	2, 11	2, 7	2, 7
17	2, 11	2, 7	2, 11
18	2, 11	2, 7	2, 7
19	2, 11	7, 10	7, 10
20	2, 7	2, 7	2,7
21	2, 7	2, 7	2, 7
22	7, 10	2, 7	7, 10
23	7, 10	7, 10	7, 10
24	7, 10	7, 10	2, 11
Runtime (s)	123	117.2	37.5
Operation cost ($)	2783.8	2855.6	2435.833

5 | CONCLUSION

In this paper, optimal risk-based scheduling of integrated power and natural gas grids with a focus on distributed EHs was proposed, which considered the reconfigurable capability in a multi-carrier energy system, for the first time. The natural gas-fired units and EHs that were equipped by CHP, gas boiler, heat pump, and thermal storage were considered as gas consumers which make links between gas and electricity carriers. The proposed scheduling was formulated as a two-stage stochastic model and conditional value at risk was implemented to manage the risk associated with strong uncertainties. The model was examined on the test system in different cases. The following major conclusions are drawn from the simulation results:

- The hourly reconfiguration while increasing the power purchased, results in gas purchased reduction, as well as operational cost reduction up to 7.82%.
- The effects of β reveal that the risk-averse operator prefers to buy power from the real-time market, while the

risk-taker operator prefers to purchase from the day-ahead market.
- Under the risk-based strategy, the gas flow rate between the main pipeline reduces while the power purchased is increased, as the value of β increases.
- As the value of β increases, the CVaR is reduced, while the expected operation cost is increased up to 14.6%. In other words, high expected operational cost is obtained at low-level risk, and vice versa.

ACKNOWLEDGEMENTS

The authors acknowledge support of the "Optimal Operation of Natural Gas and Reconfigurable Electricity Networks in presence of Connected Energy Hub to Network" project funded by Iran National Science Foundation (INSF) under Grant No. 99012662.

This project has been supported by a research grant of the University of Tabriz (number: 3622).

Nomenclature

Index

t	Index of times
g	Index of gas-fired units
n	Index of CHP units
ω	Index of scenarios
b	Index of battery energy storage units
d	Index of load
e	Index of minimum ON/OFF time limits from 1 to max{MUT_g, MDT_g}
i, j	Index of electrical buses
i'	Index of electrical bus contains energy hub
l, m	Index of NG nodes
h	Index of interconnected energy hub
bo	Index of GB units
hs	Index of heat storage
hp	Index of heat pump
tr	Index of transformer
ij	Index of electrical line between i and j buses
lm	Index of gas pipeline between l and m nodes
up	Upstream network
w	Index of wind turbine

Constant

NT	Number of time horizon
NU	Number of gas-fired units
NC	Number of CHP units
BO	Number of GB units
NS	Number of scenarios
B_i	Set of batteries directly connected to bus i
$D_i, D_{i'}$	Set of electrical loads directly connected to bus i and i'
G_i	Set of gas-fired units directly connected to bus i
G_l	Set of gas-fired units directly connected to gas node l
J_i	Set of electrical buses directly connected to bus i
$H_{i'}$	Set of energy hubs directly connected to bus i'
$N_{i'}$	Set of CHP units in energy hub that connected to bus i'
$Hp_{i'}$	Set of heat pump in energy hub that connected to bus i'
$Bo_{i'}$	Set of GB units in energy hub that connected to bus i'
$Hs_{i'}$	Set of heat storage in energy hub that connected to bus i'
$TR_{i'}$	Set of transformer in energy hub that connected to bus i'
H_l	Set of energy hubs directly connected to node l
M_l	Set of gas nodes directly connected to node l
D_l	Set of gas loads (gas-fired units or hub) directly connected to node l
w_i	Set of wind turbine directly connected to bus i
λ_t^G	Forecasted NG price [cent/kWh]
λ_t^D	Forecasted day-ahead power price [cent/kWh]
$G_{lm}^{line,\max}$	Maximum gas flow rate between gas nodes l and m [m^3/h]
$GM^{\max}$	Maximum amount of purchased gas from gas market [m^3/h]
$G_h^{\max}$	Maximum NG consumed by energy hub [m^3/h]
C_{lm}	Coefficient of gas pipelines function of length and other characteristics of pipeline
C_{lm}	Switching action cost [cent]
$F(P_g)^{\max}$	Max gas consumed by GF unit [kWh]
eh^{ch}, eh^{dis}	Charging/discharging efficiency of heat storage
$HS^{hs,\min}$, $HS^{hs,\max}$	Min/max value of heat storage [kWh]
$H^{hs,ch,\min}$, $H^{hs,ch,\max}$	Min/max value of charging for heat storage [kW]
$H^{hs,dis,\min}$, $H^{hs,dis,\max}$	Min/max value of discharging for heat storage [kW]
$H^{bo,\min}$, $H^{bo,\max}$	Min/max heat generated by GB unit [kW]
NLI_{IS}	Number of close switches
NLI_{LP}	Number of switches in loop
$SOC_b^{\min}$, $SOC_b^{\max}$	Min/max state of charge of battery [%]
$SOC_{b,int}$	Initial state of charge of battery [%]
SUC_g/SDC_g	Start-up/shut-down cost of gas-fired unit g[cent/kW]

η_b^{ch}/η_b^{dis} Charging/discharging efficiency of battery

$P_b^{ch,\min}$ $P_b^{ch,\max}$ Minimum/maximum value of charging for battery [kW]

$P_b^{dis,\min}$ $P_b^{dis,\max}$ Minimum/maximum value of discharging for battery [kW]

$P_g^{\min}/P_g^{\max}$ Minimum/maximum active power generated by gas-fired unit*g* [kW]

$Q_g^{\min}/Q_g^{\max}$ Minimum/maximum reactive power generated by gas-fired unit*g*[kVar]

$P^{hp,\max}$ Maximum active power consumed by heat pump [kW]

$Q^{hp,\max}$ Maximum reactive power consumed by heat pump [kVar]

$P^{tr,\max}$ Maximum internal active power consumption by transformer [kW]

$Q^{tr,\max}$ Maximum internal reactive power consumption by transformer [kVar]

$P_n^{\min}/P_n^{\max}$ Minimum/maximum active power generated by CHP unit [kW]

$Q_n^{\min}/Q_n^{\max}$ Minimum/maximum reactive power generated by CHP unit [kVar]

MUT_g/MDT_g Minimum up / down time of gas fired unit [hour]

R_g^{up}/R_g^{dn} Ramp-up/ramp-down of gas-fired unit [kW]

R_n^{up}/R_n^{dn} Ramp-up/ramp-down of CHP unit [kW]

B_{ij} Real part of admittance matrix of electrical network [p.u.]

G_{ij} Imaginary part of admittance matrix of electrical network [p.u.]

$S_{ij}^{\max}$ Maximum kVA capacity of feeder between *i* and *j* buses [kVA]

$V_i^{\min}/V_i^{\max}$ Minimum/ maximum voltage of electrical bus [p.u.]

$\rho_l^{\min}/\rho_l^{\max}$ Minimum/ maximum pressure of gas node [p.u.]

Variables

EM_t Active power purchased from day-ahead market [kW]

$GM_{t,\omega}$ Gas purchased from the gas market [kW]

$G_{lm,t,\omega}^{line}$ Gas flow rate between gas nodes *l* and *m* [m^3/h]

$G_{d,t,\omega}$ Gas demand (gas-fired units or EHs) [m^3/h]

$G_{b,t,\omega}$ Energy hub gas consumed [m^3/h]

$H_{d,t,\omega}$ Thermal demand [kW]

$HS_{t,\omega}^{bs}$ Heat storage capacity [kWh]

$H_{n,t,\omega}$ Generated heat by CHP unit [kW]

$H_{t,\omega}^{bo}$ Generated heat by GB [kW]

$H_{t,\omega}^{bs,dis}/H_{t,\omega}^{bs,ch}$ Heat discharging/charging of heat storage [kW]

$I_{t,\omega}^{bs,dis}/I_{t,\omega}^{bs,ch}$ Binary variable for discharging/charging mode of heat storage

$K_{i,j,t,\omega}$ Binary variable for switch status between bus *i* and *j*

$N_{k,t,\omega}^{sw}$ Number of switching action

$P_{g,t,\omega}$ Active power generated by gas-fired [kW]

$P_{b,t,\omega}^{dis}/P_{b,t,\omega}^{ch}$ Power discharging/ charging value of battery [kW]

$P_{n,t,\omega}$ Active power generated by CHP unit [kW]

$P_{t,\omega}^{hp}$ Active power consumed by heat pump [kW]

$P_{w_i,t,\omega}$ Active power generated by wind turbine [kW]

$P_{d,t,\omega}$ Other active power demand not supplied by EH [kW]

$P_{d,t,\omega}^{hub}$ Active electrical demand supplied by EH [kW]

$PF_{ij,t,\omega}$ Active power flow in feeder between *i* and *j* buses [kW]

$P_{b,t,\omega}^{hub}$ Active power of energy hub [kW]

$P_{t,\omega}^{tr}$ Active power consumption by transformer [kW]

$\rho_{l,t,\omega}/\rho_{m,t,\omega}$ Gas pressure at node *l*/ *m* [p.u.]

$Q_{g,t,\omega}$ Reactive power generated by gas-fired [kVar]

QEM_t Reactive power from/to the upstream network injected/issued in day-ahead [kVar]

$QRM_{t,\omega}$ Reactive power from/to the upstream network injected/issued in real-time [kVar]

$Q_{w_i,t,\omega}$ Reactive power generated by wind turbine [kVar]

$Q_{d,t,\omega}$ Other reactive load demand not supplied by EH [kVar]

$Q_{d,t,\omega}^{hub}$ Reactive load demand supplied by EH [kVar]

$QF_{ij,t,\omega}$ Reactive power flow in feeder between bus *i* and *j* [kVar]

$Q_{b,t,\omega}^{hub}$ Reactive power of energy hub [kVar]

$Q_{t,\omega}^{tr}$ Reactive power of transformer [kVar]

$Q_{n,t,\omega}$ Reactive power generated by CHP unit [kVar]

$Q_{t,\omega}^{hp}$ Reactive power consumed by heat pump [kVar]

OF Objective function

$RM_{t,\omega}$ Power purchased from real-time market [kW]

$\lambda_{t,\omega}^{R}$ Real-time power price [cent/kWh]

$SOC_{b,t+1,\omega}$, $SOC_{b,t,\omega}$ State of charge of battery

$SU_{g,t}/SD_{g,t}$ Start-up/shut-down cost gas-fired [cent/kWh]

$SU_{n,t}/SD_{n,t}$ Start-up/shut-down cost CHP [cent/kWh]

S_{up} kVA power exchanged with upstream network [kVA]

$V_{i,t,\omega}/V_{j,t,\omega}$ Voltage magnitude at bus *i*/ *j* [p.u.]

$x^{dis}_{b,t,\omega}/x^{ch}_{b,t,\omega}$	Binary variable for discharging/charging mode of battery
x^{bo}_{t}	Binary variable for GB unit
$u_{n,t}$	Binary variable for CHP unit
$u_{g,t}/u_{g,t-1}$	Binary variable for gas-fired unit
π_{ω}	Scenario probability
$\delta_{i,t,\omega}/\delta_{j,t,\omega}$	Voltage angle of bus i/j [rad]

ORCID

Mohammad Hemmati https://orcid.org/0000-0002-6661-3059
Mehdi Abapour https://orcid.org/0000-0003-0241-7021
Behnam Mohammadi-Ivatloo https://orcid.org/0000-0002-0255-8353
Amjad Anvari-Moghaddam https://orcid.org/0000-0002-5505-3252

REFERENCES

1. Conti, J.J., et al.: Annual energy outlook 2014. US Energy Information Administration 2 (2014)
2. Nosratabadi, S.M., Jahandide, M., Nejad, R.K.: Simultaneous planning of energy carriers by employing efficient storages within main and auxiliary energy hubs via a comprehensive milp modeling in distribution network. J. Storage Mater. 30, 101585 (2020)
3. Mirzaei, M.A., et al.: A novel hybrid two-stage framework for flexible bidding strategy of reconfigurable micro-grid in day-ahead and real-time markets. Int. J. Electr. Power Energy Syst. 123, 106293 (2020)
4. Giglio, E., et al.: Synthetic natural gas via integrated high-temperature electrolysis and methanation: Part I—energy performance. J. Storage Mater. 1, 22–37 (2015)
5. Guo, B., Ghalambor, A.: Natural Gas Engineering Handbook. Elsevier, New York (2014)
6. Wong, P., Larson, R.: Optimization of natural-gas pipeline systems via dynamic programming. IEEE Trans. Autom. Control 13(5), 475–481 (1968)
7. Andre, J., Bonnans, F., Cornibert, L.: Optimization of capacity expansion planning for gas transportation networks. Eur. J. Oper. Res. 197(3), 1019–1027 (2009)
8. Mirzaei, M.A., et al.: Robust flexible unit commitment in network-constrained multicarrier energy systems. IEEE Syst. J. (2020)
9. Zlotnik, A., et al.: Coordinated scheduling for interdependent electric power and natural gas infrastructures. IEEE Trans. Power Syst. 32(1), 600–610 (2016)
10. Liu, F., Bie, Z., Wang, X.: Day-ahead dispatch of integrated electricity and natural gas system considering reserve scheduling and renewable uncertainties. IEEE Trans. Sustainable Energy 10(2), 646–658 (2018)
11. Liu, C., Shahidehpour, M., Wang, J.: Coordinated scheduling of electricity and natural gas infrastructures with a transient model for natural gas flow. Chaos: An Interdisciplinary Journal of Nonlinear Science 21(2), 025102 (2011)
12. Bai, J., et al.: Interdependence of electricity and heat distribution systems coupled by an aa-caes-based energy hub. IET Renewable Power Gener. 14(3), 399–407 (2019)
13. Ghasemi, H., et al.: Milp model for integrated expansion planning of multi-carrier active energy systems. IET Gener. Transm. Distrib. 13(7), 1177–1189 (2018)
14. Correa-Posada, C.M., Sánchez.Martín, P.: Integrated power and natural gas model for energy adequacy in short-term operation. IEEE Trans. Power Syst. 30(6), 3347–3355 (2014)
15. Khaligh, V., Anvari-Moghaddam, A.: Stochastic expansion planning of gas and electricity networks: a decentralized-based approach. Energy 186, 115889 (2019)
16. Bao, Z., Ye, Y., Wu, L.: Multi-timescale coordinated schedule of interdependent electricity-natural gas systems considering electricity grid steady-state and gas network dynamics. Int. J. Electr. Power Energy Syst. 118, 105763 (2020)
17. Xu, X., et al.: Dynamic modeling and interaction of hybrid natural gas and electricity supply system in microgrid. IEEE Trans. Power Syst. 30(3), 1212–1221 (2014)
18. Wu, H., et al.: Demand response exchange in the stochastic day-ahead scheduling with variable renewable generation. IEEE Trans. Sustainable Energy 6(2), 516–525 (2015)
19. Liu, W., et al.: Optimal scheduling of multi-source microgrid considering power to gas technology and wind power uncertainty. Energy Procedia 143, 668–673 (2017)
20. Liu, W., et al.: Day-ahead optimal operation for multi-energy residential systems with renewables. IEEE Trans. Sustainable Energy 10(4), 1927–1938 (2018)
21. Ding, T., Hu, Y., Bie, Z.: Multi-stage stochastic programming with nonanticipativity constraints for expansion of combined power and natural gas systems. IEEE Trans. Power Syst. 33(1), 317–328 (2017)
22. Mohammadi, M., et al.: Energy hub: From a model to a concept–a review. Renewable Sustainable Energy Rev. 80, 1512–1527 (2017)
23. Liu, T., Zhang, D., Wu, T.: Standardised modelling and optimisation of a system of interconnected energy hubs considering multiple energies—electricity, gas, heating, and cooling. Energy Convers. Manage. 205, 112410 (2020)
24. Lu, Q., et al.: Optimal household energy management based on smart residential energy hub considering uncertain behaviors. Energy 195, 117052 (2020)
25. Karamdel, S., Moghaddam, M.P.: Robust expansion co-planning of electricity and natural gas infrastructures for multi energy-hub systems with high penetration of renewable energy sources. IET Renewable Power Gener. 13(13), 2287–2297 (2019)
26. Fathtabar, H., Barforoushi, T., Shahabi, M.: Dynamic long-term expansion planning of generation resources and electric transmission network in multi-carrier energy systems. Int. J. Electr. Power Energy Syst. 102, 97–109 (2018)
27. Xu, D., et al.: Distributed multi-energy operation of coupled electricity, heating and natural gas networks. IEEE Trans. Sustainable Energy 11(4), 2457–2469 (2019)
28. Dolatabadi, A., Mohammadi-Ivatloo, B.: Stochastic risk-constrained scheduling of smart energy hub in the presence of wind power and demand response. Appl. Therm. Eng. 123, 40–49 (2017)
29. Bai, J., et al.: Interdependence of electricity and heat distribution systems coupled by an aa-caes-based energy hub. IET Renewable Power Gener. 14(3), 399–407 (2019)
30. Hemmati, M., Ghasemzadeh, S., Mohammadi-Ivatloo, B.: Optimal scheduling of smart reconfigurable neighbour micro-grids. IET Gener. Transm. Distrib. 13(3), 380–389 (2018)
31. Khomami, M.S., et al.: Bi-level network reconfiguration model to improve the resilience of distribution systems against extreme weather events. IET Gener. Transm. Distrib. 13(15), 3302–3310 (2019)
32. Hemmati, M., et al.: Risk-based optimal scheduling of reconfigurable smart renewable energy based microgrids. Int. J. Electr. Power Energy Syst. 101, 415–428 (2018)
33. Zhan, J., et al.: Switch opening and exchange method for stochastic distribution network reconfiguration. IEEE Trans. Smart Grid 11(4), 2995–3007 (2020)
34. Wang, Y., et al.: Transactive energy trading in reconfigurable multi-carrier energy systems. J. Mod. Power Syst. Clean Energy 8(1), 67–76 (2019)
35. Hemmati, M., et al.: Optimal chance-constrained scheduling of reconfigurable microgrids considering islanding operation constraints. IEEE Syst. J. 14(4), 5340–5349 (2020)
36. Moazeni, S., Miragha, A.H., Defourny, B.: A risk-averse stochastic dynamic programming approach to energy hub optimal dispatch. IEEE Trans. Power Syst. 34(3), 2169–2178 (2018)
37. Mirzaei, M.A., et al.: Two-stage robust-stochastic electricity market clearing considering mobile energy storage in rail transportation. IEEE Access 8, 121780–121794 (2020)
38. Vahedipour-Dahraie, M., et al.: Risk-averse probabilistic framework for scheduling of virtual power plants considering demand response

and uncertainties. Int. J. Electr. Power Energy Syst. 121, 106126 (2020)
39. Ahrabi, M., et al.: Evaluating the effect of electric vehicle parking lots in transmission-constrained ac unit commitment under a hybrid IGDT-stochastic approach. Int. J. Electr. Power Energy Syst. 125, 106546 (2021)
40. Hemmati, M., et al.: Optimal operation of integrated electrical and natural gas networks with a focus on distributed energy hub systems. Sustainability 12(20), 8320 (2020)
41. Shams, M.H., et al.: Risk-averse optimal operation of multiple-energy carrier systems considering network constraints. Electr. Power Syst. Res. 164, 1–10 (2018)
42. Salkuti, S.R.: Risk-based optimal operation of hybrid power system using multiobjective optimization. Int. J. Green Energy 17(13), 853–863 (2020)
43. Reddy, S.S., et al.: Joint energy and spinning reserves market clearing for wind-thermal power system incorporating wind generation and load forecast uncertainties. IEEE Syst. J. (2015) 9(1), 152–164

How to cite this article: Hemmati, M., et al.: Risk-based optimal operation of coordinated natural gas and reconfigurable electrical networks with integrated energy hubs. *IET Renew. Power Gener.* 1–17 (2021). https://doi.org/10.1049/rpg2.12189